



# Morphological convexity measures for terrestrial basins derived from digital elevation models

Sin Liang Lim <sup>a,\*</sup>, B.S. Daya Sagar <sup>b</sup>, Voon Chet Koo <sup>a</sup>, Lea Tien Tay <sup>c</sup>

<sup>a</sup> Faculty of Engineering and Technology, Melaka Campus, Multimedia University, Jalan Ayer Keroh Lama, 75450 Melaka, Malaysia

<sup>b</sup> Systems Science and Informatics Unit (SSIU), Indian Statistical Institute-Bangalore Centre, 8th Mile, Mysore Road, RV College PO, Bangalore 560059, India

<sup>c</sup> School of Electrical and Electronic Engineering, Universiti Sains Malaysia, Engineering Campus, Nibong Tebal, 14300 Penang, Malaysia

## ARTICLE INFO

### Article history:

Received 26 April 2010

Received in revised form

12 October 2010

Accepted 15 October 2010

Available online 12 November 2010

### Keywords:

Convexity measures

Spatial variability

Mathematical morphology

## ABSTRACT

Geophysical basins of terrestrial surfaces have been quantitatively characterized through a host of indices such as topological quantities (e.g. channel bifurcation and length ratios), allometric scaling exponents (e.g. fractal dimensions), and other geomorphometric parameters (channel density, Hack's and Hurst exponents). Channel density, estimated by taking the ratio between the length of channel network ( $L$ ) and the area of basin ( $A$ ) in planar form, provides a quantitative index that has hitherto been related to various geomorphologically significant processes. This index, computed by taking the planar forms of channel network and its corresponding basin, is a kind of convexity measure in the two-dimensional case. Such a measure – estimated in general as a function of basin area and channel network length, where the important elevation values of the topological region within a basin and channel network are ignored – fails to capture the spatial variability between *homotopic* basins possessing different altitude-ranges. Two types of convexity measures that have potential to capture the terrain elevation variability are defined as the ratio of (i) length of channel network function and area of basin function and (ii) areas of basin and its convex hull functions. These two convexity measures are estimated in three data sets that include (a) synthetic basin functions, (b) fractal basin functions, and (c) realistic digital elevation models (DEMs) of two regions of peninsular Malaysia. It is proven that the proposed convexity measures are altitude-dependent and that they could capture the spatial variability across the *homotopic* basins of different altitudes. It is also demonstrated on terrestrial DEMs that these convexity measures possess relationships with other quantitative indexes such as fractal dimensions and complexity measures (roughness indexes).

© 2010 Elsevier Ltd. All rights reserved.

## 1. Introduction

Conventional geomorphometric quantities (e.g. Horton, 1945; Strahler, 1964) were previously computed based on the details available from two-dimensional topographic map-sources in order to quantitatively characterize terrestrial surfaces. These geomorphometric quantities include a host of indices such as channel bifurcation and length ratios, channel density, and Hack's and Hurst exponents. Length of the channel network divided by the area of the basin in planar forms provides a quantitative index termed as channel density, which is defined here as a convexity measure of the basin in two dimensions. In the context of hydrogeology, the channel density is related to climate, geology, rainfall, erosion rate, and relief (e.g. Kirkby, 1980, 1993; Howard, 1997; Schumm et al., 1987; Montgomery and Dietrich, 1989, 1994). During the last two decades, several techniques

have emerged to quantitatively characterize terrestrial surfaces. These geometrically rigorous techniques, to name a few, originated from fractal geometry (Mandelbrot, 1982) and mathematical morphological (Serra, 1982) concepts. Their potential were demonstrated in digital elevation models (DEMs) derived from multiscale multitemporal remotely sensed data acquired through various sensing mechanisms. In subsequent investigations, the importance of digital elevation models (DEMs) in deriving quantitative geomorphological indicators (e.g. roughness characteristics, channel densities) that exhibit rich scale-invariant properties is greatly realized (Tarboton et al., 1992; Tarboton, 1997; Tarboton and Ames, 2001). While explaining the importance of DEM analysis in understanding the landscape state and process interactions, Tucker and Bras (1998) have shown how drainage density is related to topographic relief through the sign of the predicted relationship between drainage density and relief. From their results, a positive sign of the predicted relationship implies low topographic relief, while a negative sign of the predicted relationship implies high topographic relief. Tucker et al. (2001) proposed to map drainage density using two scalar fields, namely: the local hillslope length from any unchanneled site to the channel network and the local hillslope

\* Corresponding author. Tel.: +60 3 8312 5367; fax: +60 3 8318 3029.

E-mail addresses: [lim.sin.liang@mmu.edu.my](mailto:lim.sin.liang@mmu.edu.my), [sinliang\\_lim@yahoo.com](mailto:sinliang_lim@yahoo.com) (S.L. Lim).

length to the valley networks. All these studies addressed the drainage density as either main topics or the subtopics of studies on fluvial basins. In a recent study, Marani et al. (2003) addressed the problem of estimation of drainage density of tidal basins.

No watershed or basin is fully convex due to the presence of valleys and ridges. A parameter that computes the degree of convexity of a watershed is the convexity measure, which is in some way related to channel (drainage) density estimated by taking two basic measures, the planar basin's area and the planar network's length, as major inputs. Drainage density, according to Horton (1945), is defined dimensionally as the ratio of the total network length to its watershed area,  $DD=L/A$ , where  $L$  and  $A$ , respectively, denote length of network and area of the basin. The basic parameters required to estimate this measurement heavily rely on plan-forms of basin and network. The plan-view of the basin and its corresponding network provide the 2-dimensional flat basin and the network. Hence, this definition, from the point of convexity measure, has a limitation as it cannot capture the elevation variability among different drainage basins. The maps of drainage density do not carry information on terrain morphology as high drainage density may occur in flat, low relief basins as well as in mountainous, high relief basins. This type of estimation is of limited use as it cannot capture the basic difference involved in two seemingly alike basins and their networks over a planar view. It is intuitively true that the convexity measures of the seemingly alike (*homotopic*) basins with varied altitudes should be different in such a way that it reflects the changes in the altitudes involved. Our proposed method shows distinction between the cases that belong to two altitude-regions. Such a distinction could be shown through alternative measures that we proposed in this paper. Here the inputs are represented as 3-dimensional functions and not as planar sets.

The three significant parameters, which require morphological quantities in the form of functions, include (i) basin function,

(ii) channel network function, and (iii) convex hull of basin function. These three functions are respectively denoted as  $f(x,y)$ ,  $g(x,y)$ , and  $CH(f)$ . The two alternative measures that we propose in this paper for estimation of the convexity measures are mainly based on estimations of the length of network function and that of areas under basin and its convex hull functions. The basic measures to compute these convexity measures include the basin area  $A(f)$ , the length of the networks  $A(g)$ , and the area of convex hull of basin  $A[CH(f)]$ . The convex hull of the basin is the smallest convex function containing  $f$  such that  $A(f) < A[CH(f)]$ . These two convexity measures include (i) ratio between the length of channel network function  $A(g)$  and the area of basin function  $A(f)$  and (ii) ratio between the area of basin function  $A(f)$  and the area of its corresponding convex hull  $A[CH(f)]$ .

## 2. Data used and their specifications

We implement our proposed methods with two types of data, namely synthetic DEMs (simple synthetic functions and fractal basin functions) and real world DEMs. These synthetic DEMs include: (i) rectangle-like discrete synthetic basin functions, denoted as basin functions  $f_1$  and  $f_2$ , respectively, shown in (Fig. 1a and b), and (ii) fractal basin functions, indicated as basin functions  $f_3$  and  $f_4$  depicted in (Fig. 2a and b). In these basin functions, each discrete element with a specific numerical value represents the elevation at spatial coordinates  $(x, y)$ . These two pairs of synthetic basins possess a similar spatial organization of networks, but it is obvious that they belong to two different altitudes. It is heuristically true that these two pairs of functions possess different spatial organizations of hillslopes, and thus different geomorphic processes, as they belong to different categories of elevations. The plan views of the basin and its

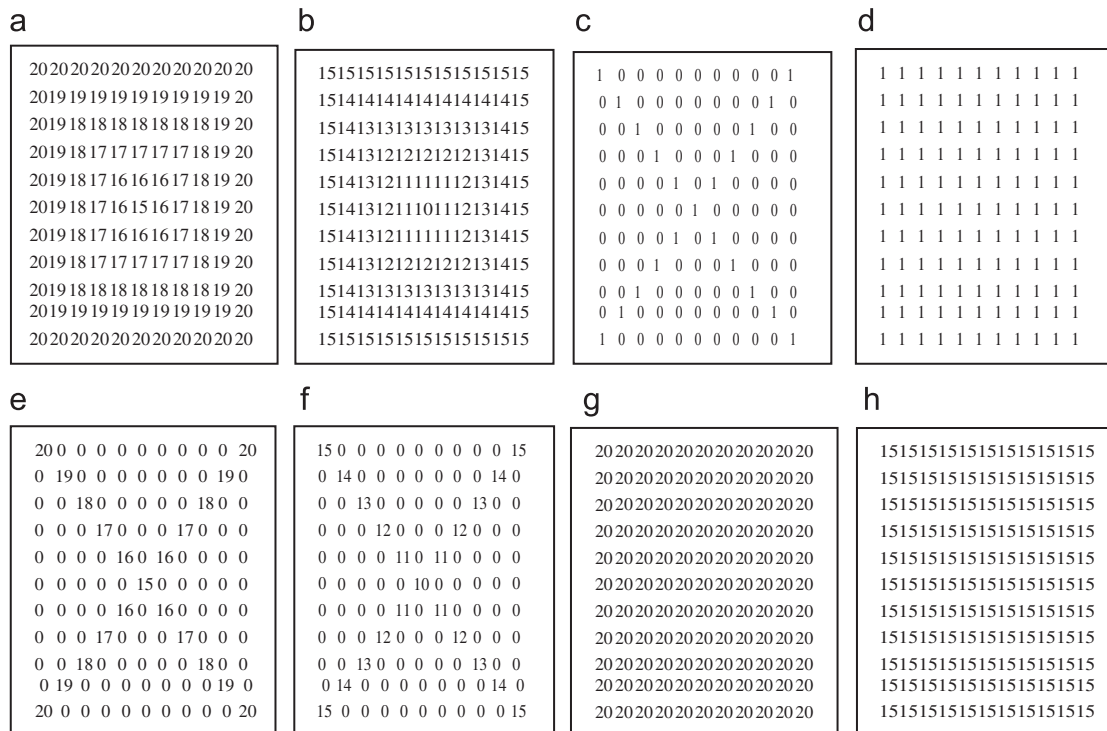


**Fig. 1.** (a, b) Synthetic basins depicted as discrete functions, in which the higher the value the higher is the elevation. In turn, these functions are treated as two different basins with two different altitudes set-up, (c) typical planar form of drainage network that summarizes the connectivity and shape of these two functions. It is extracted by following morphology based transformations (e.g. Sagar et al., 2000). In Fig. 1c, 1s are channel subsets and 0s represent non-channel regions, (d) planar form of the basin areas of the two synthetic basin functions, threshold value employed is  $< 20$  and  $< 15$  (respectively, for two functions shown in (a, b)) and converted into 1s, and 0s for other value(s), (e, f) the elevation values from basin functions shown in Fig. 1a, b corresponding to the channel subsets shown in Fig. 1c, and (g, h) convex hulls of two synthetic basin functions constructed according to a procedure due to Soille (1998). The step-wise procedure to construct the convex hull is explained in Section 3.2 and Fig. 6.

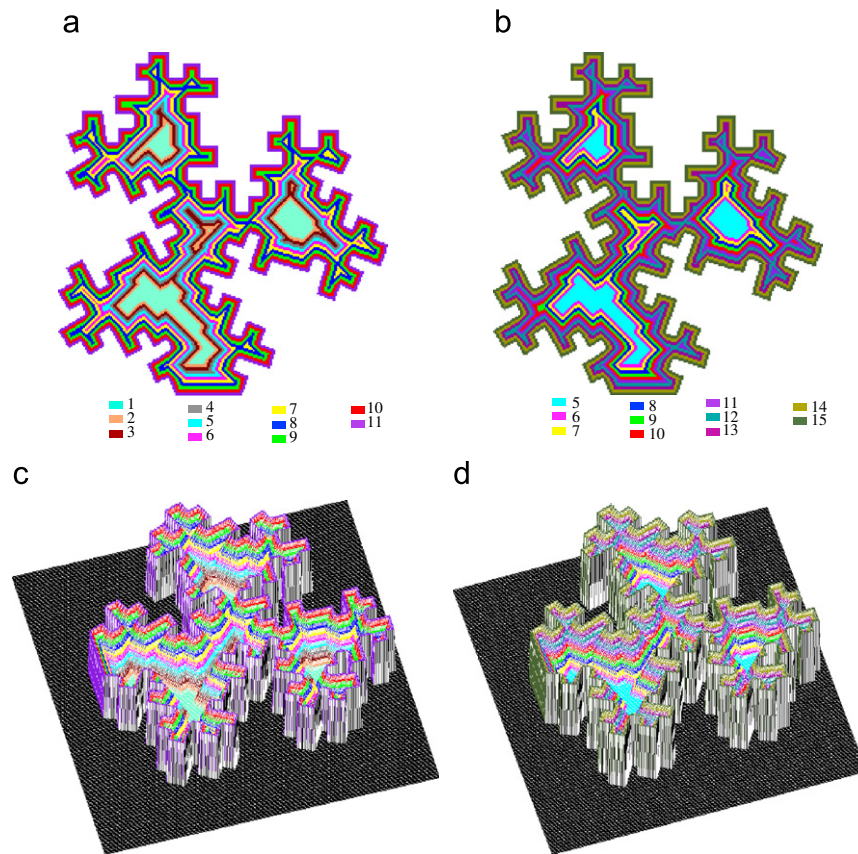


Fig. 2. (a, b) Fractal basin functions with elevation ranges of 1–11 and 5–15 and (c, d) 3-D representation of fractal basin functions shown in (a, b).

corresponding channel network are like sets that are decomposed from a function ( $f$ ), where its landscape is represented by the digital elevation model (DEM) (e.g. Fig. 2c–d).

DEM is denoted as a function represented by a non-negative 2-D sequence  $f(m, n)$ , which assumed  $I+1$  possible intensity (elevation) values:  $i=0, 1, 2, \dots, I$ . The data range in synthetic data is within the interval from 0 to 255 ( $I=255$ ) elevations. The function,  $f$ , is discrete, defined on a (rectangular) subset of the discrete plane  $Z^2$ . The higher the intensity value, the higher is the topographic elevation, and vice versa. Fractal basin functions,  $f_3$  and  $f_4$ , are simulated by transforming a binary fractal shape into fractal basin functions (Fig. 2a, b) that mimic digital elevation models. The transformation process is performed in the following way. Firstly, the binary fractal shape, whose network follows the Hortonian laws of morphometry (Sagar et al., 2001), is subjected to iterative morphologic erosions by means of the structuring of an element of octagonal shape (Sagar and Tien, 2004; Chockalingam and Sagar, 2005). Each eroded version is coded with a specific color to denote different elevation level. Eleven iterative erosions are performed to transform binary fractal shape of size  $256 \times 256$  into eleven eroded versions. Each eroded version is color-coded separately to generate two fractal basin functions (Fig. 2a, b). The color-numbers employed to respectively denote these two functions are in the ranges of 1–11 and 5–15. These ranges are used to show that these two *homotopically* similar synthetic fractal basin functions with similar geometric organizations possess different altitude-ranges. These two functions are also shown in 3-D representation (Fig. 2c, d). The real world DEMs correspond to the topographic synthetic aperture radar (TOPSAR) DEMs of the Cameron Highlands (Fig. 4a) and those of the Petaling regions (Fig. 4b) of Malaysia from Tay et al. (2007). The Cameron Highlands study area is enclosed by latitude  $4^\circ 31' - 4^\circ 36' N$  and longitude  $101^\circ 15' - 101^\circ 20' E$ , while the Petaling

region is enclosed by latitude  $2^\circ 59' - 3^\circ 02' N$  and longitude  $101^\circ 37' - 101^\circ 40' E$ . Cameron Highlands is a highland region situated in the state of Perak, Malaysia. It is a hilly terrain with elevation range in between 400 and 1800 m. The Petaling region is located in Selangor state in Malaysia, and it is comparatively flat with an altitude of not more than 215 m. The Cameron Highlands, DEM covers an area of  $900 \times 900$  pixels with 10 m resolution, while Petaling's DEM covers a region of  $750 \times 800$  pixels with 5 m resolution. Fourteen sub-basins were demarcated from the DEMs of Cameron Highlands and those of the Petaling regions (Fig. 4a and b). Each of the 14 sub-basins has different values of  $I$ , depending on its maximum altitude. The Cameron Highlands sub-basins are high altitude basins, whereas the Petaling sub-basins have relatively lower altitudes; hence, the value  $I$  in Cameron Highlands sub-basins is generally greater than that of the Petaling sub-basins. For instance, basin 1 (of Cameron Highlands region) has a value of  $I$  of 1280 m, while basin 8 (of Petaling region) has maximum elevation (and thus  $I$ ) of 208 m.

### 3. Methodology

In this section, we will briefly discuss the (i) derivation of a channel network from a basin function, (ii) derivation of a convex hull of a basin function, and (iii) area estimations of functions and convexity measure computation.

#### 3.1. Derivation of a channel network from a basin function

Drainage network and drainage basins were delineated from the DEMs via various methods (O'Callaghan and Mark, 1984; Jenson and Domingue, 1988; Tarboton et al., 1991; Band, 1993;

Sagar et al., 2000; Lindsay, 2005). In this paper, the channel network (e.g. Fig. 1c) is isolated from DEM via the (i) threshold decomposition of the basin function into threshold elevation sets, (ii) isolation of channel subsets through skeletonization operations from threshold elevation sets, (iii) subtraction of channel subsets from immediate higher level threshold elevation sets, and (iv) composition of channel subsets obtained at step (iii) is superposed on the basin function (e.g. Fig. 1a and b) to perform the maximum ( $\vee$ ) operation between the network (subsets derived in the form of a planar set) and their corresponding points from the basin function. Such maxima form the network function (e.g. Fig. 1e–f). This method of obtaining the network function is applicable in both synthetic DEMs and real world DEMs of fluvial and tidal basins. The planar forms of networks extracted from fractal function (Fig. 2a, b) and real world DEMs (Fig. 4a, b) obtained by following an approach due to Sagar et al. (2000) are shown in Figs. 3a, 4c and d. As the procedure to extract channel networks from DEM is well established by various methods, we will not further elaborate it here. Besides, since the focus of this paper is not on channel network extraction, the detailed procedure of extracting the channel network is omitted to avoid confusion.

### 3.2. Derivation of a convex hull of a basin function

A typical example of a function and its convex hull include a bowl with open end (Fig. 5a) and a bowl with a closed lid (Fig. 5b). As another example, if the cloud surface is considered to be a function, then its corresponding convex hull will be a blanket-like cover (Lim and Sagar, 2008). We derive the convex hull of a basin function by following an approach credited to Soille (1998). This approach to generate convex hull requires two steps: (i) transformation of a basin via closings using half planes of various directions and (ii) applying a point-wise minimum ( $\wedge$ ) operation between all versions of closing generated by half planes in all possible directions. The two-step process of convex hull,  $CH(f)$ , construction is shown as  $CH(f) = \bigwedge_{\theta} [\phi_{\pi_{\theta}^+}(f) \wedge \phi_{\pi_{\theta}^-}(f)]$ , where  $(\pi_{\theta}^+)^c = \pi_{\theta}^-$  denotes two half planes at the orientation  $\theta$ , and  $\phi(f)$  represents the closing of a basin function  $f$ . A more precise convex hull can be obtained by increasing the number of directions of half planes. For better comprehension, the generation of convex hull on a synthetic basin function of size  $3 \times 3$  is illustrated in Fig. 6. The maximum value of the column before the first column is considered to be zero. Fig. 6a is the input function, while Fig. 6b–d depicts three required translations computed by

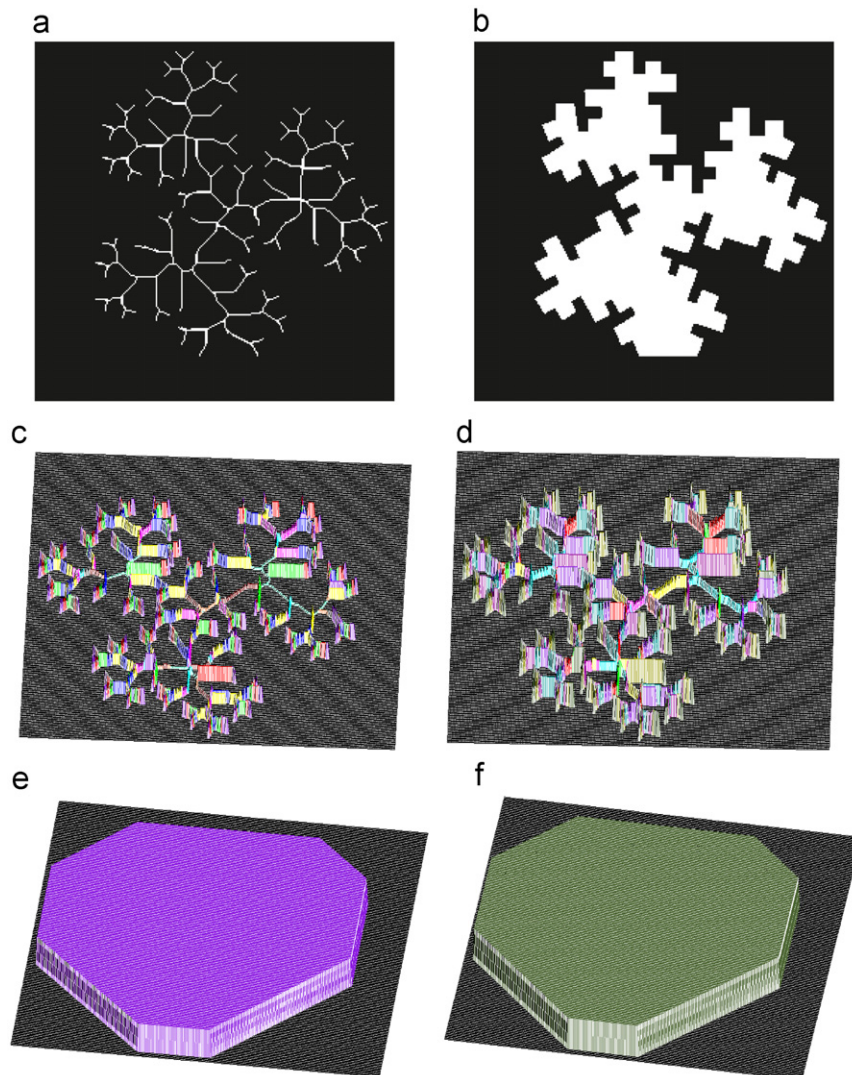


**Fig. 3.** (a) Planar view of the network that represents channel network from both fractal basin functions, (b) planar view of the threshold basin region of both fractal basin functions, (c, d) 3-D representation of channel network functions of the two fractal basin functions, and (e, f) 3-D representation of convex hull functions of the two fractal basin functions.

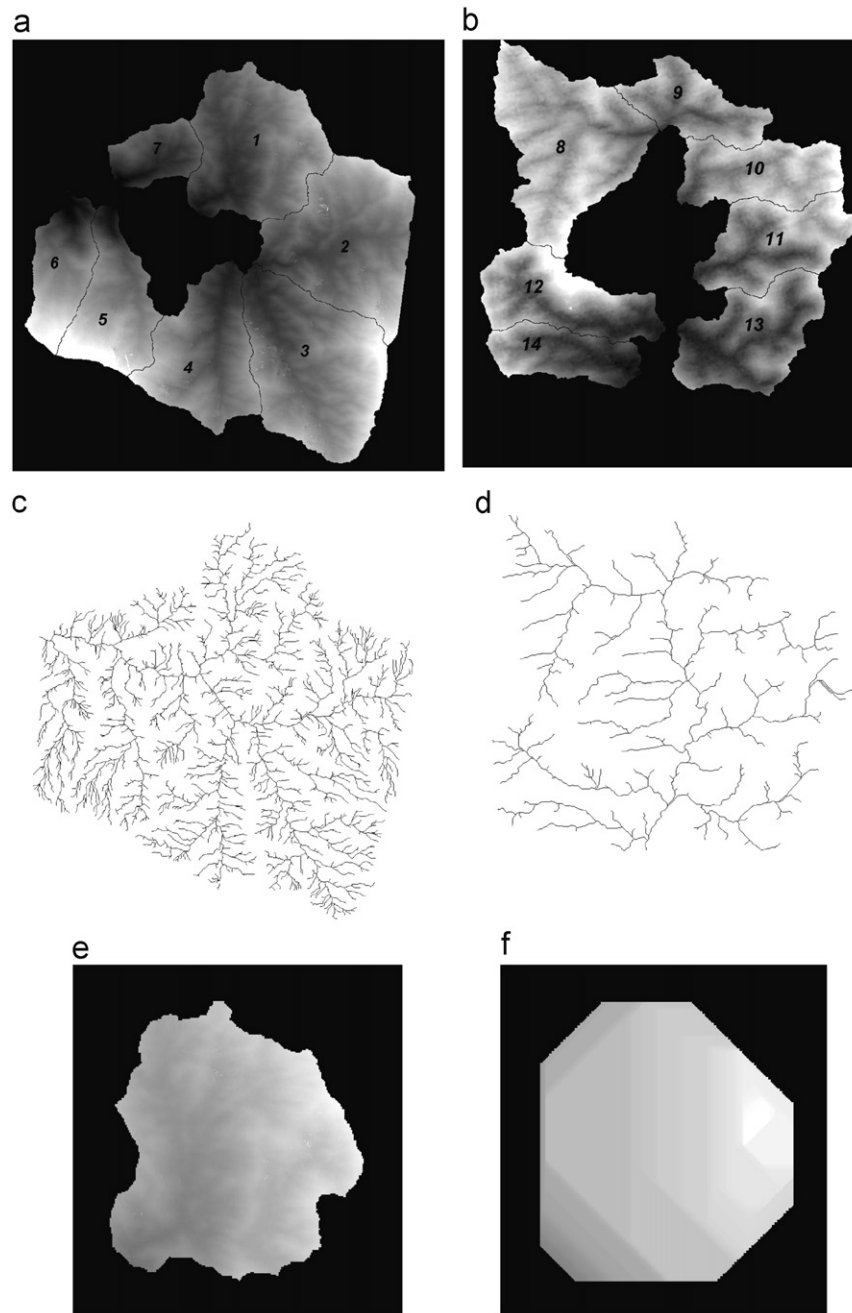


**Fig. 4.** (a) Seven delineated sub-basins of Cameron Highlands DEM, (b) seven delineated sub-basins of Petaling DEM, (c) stream networks extracted from Cameron Highlands DEM, (d) stream networks extracted from Petaling DEM, (e) DEM of basin 1, and (f) convex hull of basin 1.

following the left-vertical half-plane, and the resultant left-vertical half-plane is shown in Fig. 6e. The closings computed using the half planes of eight different directions are shown in Fig. 6(e–l). Fig. 6(e–h) shows closings of  $f$  by left (right)-vertical half planes and there by the lower (upper)-horizontal half planes, accordingly. Fig. 6(i–l) presents the closings of the remaining two pairs of orientations, namely  $3\pi/4$  and  $\pi/4$ . Finally, the infimum of Fig. 6(e–l) results in the convex hull, as shown in Fig. 6m. Half planes of eight different directions are considered to generate a sequence of closed versions of a function. These directions include vertical half planes of right and left, horizontal half planes of the top and bottom, and diagonal half planes of top-left, bottom-right, top-right, and bottom-left. To transform a function via a closing of the left-vertical half-plane in the forward direction (shown as a dark line), the half-plane is moved to the first column of the function, as

shown in Fig. 6b. The values (elevation values) in that column that coincide with the half-plane are evaluated to find out the maximum values. The first translation involved replacing all the values in that column with the maximum value, if such a value is not lesser than the value in the previous translation (Fig. 6b). This is a recursive process that is continued until the last column in that direction. Once all the columns of the function in the left-right direction have been translated via the left-vertical half-plane (Fig. 6b–d), the result is a closing function by left-vertical half-plane (Fig. 6e), and it is denoted by  $[\phi_{\pi\theta}+f]$ . Similarly, by considering the right-vertical half-plane in the direction right-left from the right most column, the values are translated until the left most column generates the closing function by means of the right-vertical half-plane (Fig. 6f). In a similar fashion, closings of the function by other half planes are generated by changing the directions. Finally, the convex hull is constructed by

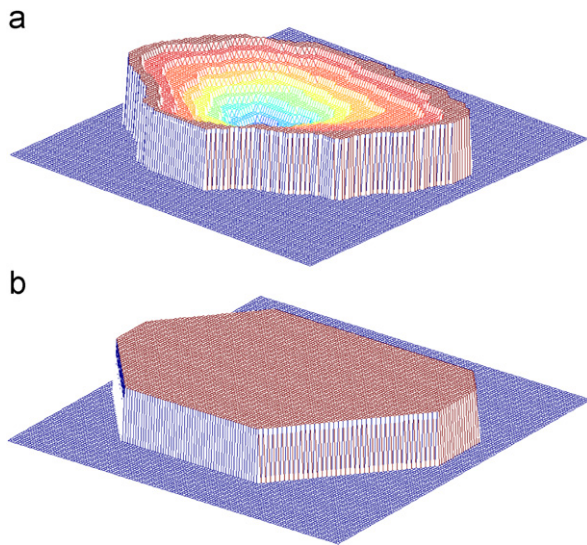


Fig. 5. (a) 3-D representation of synthetic bowl-like function and (b) 3-D representation of convex hull of synthetic bowl-like function from (a).

taking the point-wise minimum among the considered eight half-plane closings. For more details on the convex hull construction via mathematical morphology, the reader may refer to Soille (1998); Lim and Sagar (2008).

As for discrete basin functions  $f_1$  and  $f_2$  (Fig. 1a and b), the computed convex hulls are shown, respectively, in Fig. 1g and h. The reason to obtain convex hulls with only 20s and 15s, respectively, in Fig. 1g and h, is that the highest elevation values of 20s and 15s surround the outlets, which are located at the centers of the discrete basin functions and are of lower elevation values. Thus, the convex hull of these basin functions would look like “closed lids” with higher altitude values than that of the centers of the basin functions. Here, the rectangles with the highest elevation of the basins form the convex hulls of basins  $f_1$  and  $f_2$ . Similarly in case of the fractal basin functions ( $f_3$  and  $f_4$ ) shown in Fig. 2a and b, the generated convex hulls are, respectively, shown in Fig. 3e and f, where convex polygons with eight straight line segments are observed. Hence, from Fig. 1g and h and Fig. 3e and f, the hulls of the synthetic basin functions ( $f_1$  and  $f_2$ ) and fractal basin functions ( $f_3$  and  $f_4$ ) are obviously convex.

### 3.3. Area estimations for functions and convexity measure computation

The area extent of functions is estimated using  $A(f) = \sum_{(x,y)} f(x,y)$ ,  $A(g) = \sum_{(x,y)} g(x,y)$ , and  $A(CH) = \sum_{(x,y)} CH[f(x,y)]$ , according to Maragos (1989). Obviously, the area of a convex hull of a function is greater than its basin function, the area of whom is greater than its corresponding channel network function, where the relationship can be shown as  $A(CH) > A(f) > A(g)$ . For instance, the area of an image of size  $3 \times 3$  that depicts nine elevation values, shown in Fig. 6a, is 17 and the area of its convex hull (Fig. 6m) is 20. The length of the network function and the area of the basin function are significantly greater than the length of the network and the area of the basin that are depicted as planar sets, respectively. The areas of these three morphologically significant functions (i.e.  $A(f)$ ,  $A(g)$ , and  $A(CH)$ ) are evidently elevation dependent, and hence they are more appropriate for use in the estimation of the convexity measure that can capture the basic spatial variability between the basins of different altitudes. This is unlike the Hortonian drainage density computation, which does not consider the altitudes of the DEMs, and thus shows similar result with *homotopic* DEMs with different

heights, as seen in simple synthetic DEMs in Fig. 1a, b, 2a–d, the results are given in Table 1. The units in Tables 1 and 2 are the sums of pixels weighted by elevation in each pixel with ‘Areas of planar forms’ and ‘Areas of functions’. ‘Convexity measures’, ‘Normalized complexity measures’, and ‘Fractal dimensions’ are dimensionless quantities (i.e. unitless) as they define the ratio of measurements.

To compute convexity measure ( $CM_f$ ), we consider the ratio between (i) length of channel network function and area of corresponding basin function, and (ii) area of basin function and area of corresponding convex hull function, as shown in the following equations: (i)  $CM_f = A(g)/A(f)$  and (ii)  $CM_f = A(f)/A(CH)$ . Hereafter, we denote equation (i) as method-1, and equation (ii) as method-2.

## 4. Results and discussion

We demonstrate our proposed estimation first on two different simple synthetic functions ( $f_1$  and  $f_2$ ) that depict varied topographic elevations (Fig. 1a, b). Note that both basins,  $f_1$  and  $f_2$ , have a similar geometrical arrangement (that simply, both are rectangular in shape). However, basin  $f_1$  has a higher elevation range than does basin  $f_2$ : 15–20 versus 10–15. Their projections and corresponding channel networks are in 2-dimensional space (or plan views). The conventional Hortonian drainage density estimation relies on the area and the length of planar sets (e.g. basin and channel network). In a flat surface form (i.e. in planar form), the areas of both basins,  $f_1$  and  $f_2$ , are the same, with a value of 121. Similarly, the length of the planar networks extracted from corresponding basins is also the same, which is 21. Therefore, it is obvious that Horton drainage density computed with both basins,  $f_1$  and  $f_2$ , will also be the same, yielding  $(21/121) = 0.1736$ , although both basins possess different elevation ranges. This clearly shows that Horton drainage density, where  $A(g_1) = A(g_2)$  and  $A(f_1) = A(f_2)$  on plan view, respectively, denote the length of networks and area of basins on plan view, is the same with both functions  $f_1$  and  $f_2$ . Here, we show synthetic DEMs (Fig. 1a, b), in whom the spatially distributed numerical values represent topographic elevations, the higher the numerical values, the higher the elevation, and *vice versa*. The DEM is represented by the grayscale function (e.g. Fig. 1a, b), where each gray value (intensity  $I$ ) at its respective spatial coordinates  $(x,y)$  denotes the elevation value. The area is nothing but the sum of those elevation values across all the spatial positions. Such areas of the synthetic DEMs shown in Fig. 1a, b are  $A(f_1) = 2255$  and  $A(f_2) = 1650$  in pixel units, respectively. Similarly, the lengths of the channel network functions  $A(g_1)$  and  $A(g_2)$ , extracted by following morphology based algorithms (Sagar et al. 2000), are 375 and 270, respectively. The areas of convex hulls of these two functions,  $A[CH(f_1)]$  and  $A[CH(f_2)]$ , are obtained, respectively, as 2420 and 1815.

According to Horton’s definition, the drainage density of both functions  $f_1$  and  $f_2$ , is estimated to be 0.1736, which is similar to the other’s value irrespective of the elevations’ differences that exist in both functions. This approach clearly could not capture the spatial variability that is meaningful in basins with different elevations’ set-ups. However, the convexity measures computed via our two proposed methods clearly capture the spatial variability (see Table 1). Consider the two synthetic basins,  $f_1$  and  $f_2$ ; the drainage densities according to the Hortonian method yield similar values (0.1736), whereas the values obtained through method-1 are 0.1663 and 0.1636, respectively. According to method-2, these values include 0.9318 and 0.9091. The ranges of elevation values of functions  $f_3$  and  $f_4$  include 1–11 and 5–15. These ranges are used to show that these two *homotopically* similar synthetic fractal basin functions with similar geometric organizations possess different altitude-ranges. These two functions are also shown in a 3-D representation (Fig. 2c, d). The lengths of the planar network

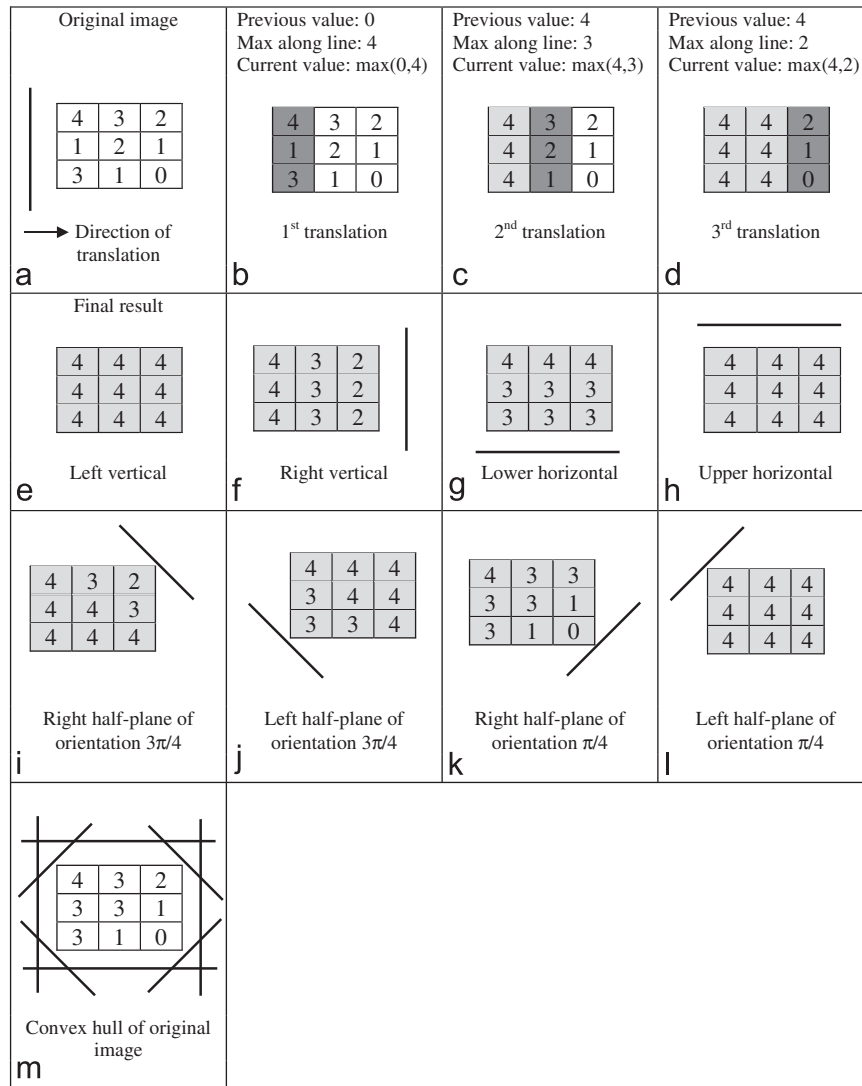


**Fig. 6.** (a)  $3 \times 3$  array depicting a synthetic basin function, (b) first translate—obtained via left-vertical half-plane by considering the previous value of the first column as 0, (c, d) second and third translates obtained via left-vertical half-plane, (e) left-vertical half-plane closing after three translations from (b to d), (f) right-vertical half-plane closing, (g) bottom–top horizontal half-plane closing, (h) top–bottom horizontal half-plane closing, (i) right half-plane (with  $3\pi/4$  orientation) closing, (j) left half-plane (with  $3\pi/4$  orientation) closing, (k) right half-plane (with  $\pi/4$  orientation) closing, (l) left half-plane (with orientation  $\pi/4$ ) closing, and (m) convex hull constructed by computing infimum values across the closing versions obtained by eight directional half planes, as shown in Fig. 6(e–l).

**Table 1**  
Comparison between drainage density and convexity measures of synthetic and fractal DEMs.

Basin	Areas of planar forms		Areas of functions			Convexity measures		
	Basin	Network	Basin	Network	Convex hull	Horton-DD	Method-1	Method-2
$f_1$	121	21	2255	375	2420	0.1736	0.1663	0.9318
$f_2$	121	21	1650	270	1815	0.1736	0.1636	0.9091
$f_3$	20,334	1838	152,844	12,132	396,814	0.0904	0.0794	0.3852
$f_4$	20,334	1838	234,180	19,484	541,110	0.0904	0.0832	0.4328

(Fig. 3a) (obtained by following the method proposed by Sagar et al. (2000)), and the areas of plan view of these two functions (Fig. 3b) are found to be the same. As a result, the Hortonian drainage densities computed for  $f_3$  and  $f_4$  are the same (0.0904) although they exhibit different altitude-ranges. In contrast, the lengths of network functions (Fig. 3c, d) and areas of basin functions and their corresponding convex hull functions (Fig. 3e, f) show distinction in the convexity measures of these two fractal basin functions. As

shown in Table 1, the convexity measures, respectively, of fractal basin functions  $f_3$  and  $f_4$  are 0.0794 and 0.0832, according to method-1, and are 0.3852 and 0.4328 according to method-2 seen early. We hypothesize that these convexity measures vary linearly with elevations of the basins. As the fractal basin function  $f_3$  has a lower altitude range than does  $f_4$ , its convexity measures computed through methods-1 and -2 are lower than that of  $f_4$ . In general, it is clearly visible in Tables 1 and 2 that values from method-1 are

**Table 2**  
Comparisons among drainage density, convexity measures, complexity measures, and fractal dimensions of realistic DEMs.

Basin	Areas of planar forms		Areas of functions			Convexity measures			Normalized complexity measures	Fractal dimensions
	Basin	Network	Basin	Network	Convex hull	Horton-DD	Method-1	Method-2		
1	71,045	3826	60,291,000	3,072,600	85,558,000	0.0539	0.0510	0.7047	0.9130	1.5141
2	77,780	4612	73,903,000	4,204,400	125,490,000	0.0593	0.0569	0.5889	0.9362	1.5506
3	84,699	4775	83,499,000	4,452,000	122,740,000	0.0564	0.0533	0.6803	0.8963	1.5814
4	55,912	3227	50,863,000	2,774,300	80,163,000	0.0577	0.0545	0.6345	0.9165	1.4692
5	41,253	2583	43,913,000	2,662,800	76,397,000	0.0626	0.0606	0.5748	0.9255	1.4519
6	31,226	2101	30,471,000	1,981,400	45,184,000	0.0673	0.0650	0.6744	0.9291	1.4776
7	19,780	1156	14,265,000	772,550	20,828,000	0.0584	0.0542	0.6849	0.9255	1.3192
8	66,824	1629	8,124,200	167,870	14,854,000	0.0244	0.0207	0.5469	0.7413	1.3140
9	25,164	588	2,605,000	46,830	5,458,100	0.0234	0.0180	0.4773	0.7788	1.2398
10	31,779	767	3,769,600	75,553	6,088,900	0.0241	0.0200	0.6191	0.8038	1.2445
11	35,805	808	3,703,100	65,298	7,216,900	0.0226	0.0176	0.5131	0.8134	1.1817
12	36,953	884	3,798,300	62,811	7,609,700	0.0239	0.0165	0.4991	0.8516	1.2946
13	40,845	933	3,189,600	50,907	6,578,400	0.0228	0.0160	0.4849	0.7921	1.1706
14	23,497	576	1,786,700	31,969	3,268,300	0.0245	0.0179	0.5467	0.7951	1.1721

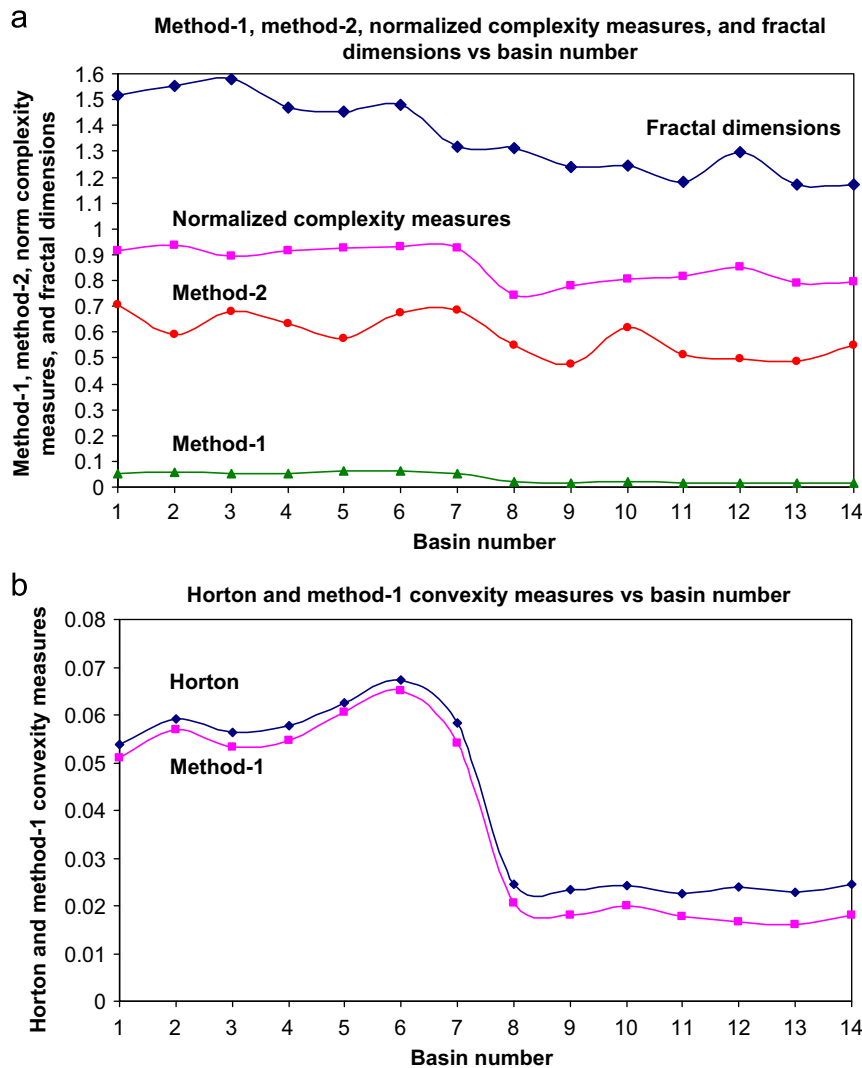


**Fig. 7.** (a) Convexity measures computed from methods-1, -2, and normalized complexity measures and fractal dimensions (via box-counting method) for all 14 basins, (b) channel densities from Horton–Strahler and method-1.

always smaller or equal to the traditional drainage density, the equal case will occur only with a basin that is flat with slightly incised valleys; the smaller the values from method-1 in

comparison with the traditional drainage density, the more will be incised the valleys. Hence, the convexity measures estimated according to the two proposed methods clearly exhibit spatial

variability of the basins, especially with those *homotopically* similar basins with different altitude-ranges.

On the basis of Table 2, we note that the Hortonian drainage density computed in case of Cameron basins have a range of 0.0539–0.0673, while in Petaling basins, the range falls within 0.0226 to 0.0245. All fourteen sub-basins have different areas of plan views, and generally the Cameron basins have larger basin areas and network lengths than do Petaling basins. Thus, the Hortonian drainage density ranges of Cameron basins are larger than those of Petaling basins. In fact, the same trend is observed also from the convexity measures obtained from methods-1 and -2. These convexity measures yield the ranges of 0.051–0.065 and 0.0160–0.0207, and 0.5748–0.7047 and 0.4773–0.6191, with Cameron basins and Petaling basins, respectively. These results match the trend observed from convexity measures computed via methods-1 and -2 in cases of fractal basin functions, i.e. the convexity measure varies with the altitude-ranges of the basins. The higher the altitude-range of the basin, the greater is the convexity measure, and *vice versa*.

To investigate the relationship between these convexity measures and complexity measures of Cameron basins and those of Petaling basins, normalized complexity measures (roughness values) are generated by following the method explained in Tay et al. (2007). Significantly, a clear distinction exists in the complexity measures between the Cameron basins and Petaling basins as the Cameron basins are highland and mountainous regions, while Petaling basins comprise relatively low and flat terrain. As such, the roughness values of Cameron basins are generally greater than that of Petaling basins. This statement is justified by the result shown in Table 2, where the ranges of normalized complexity measures of Cameron basins are 0.8963–0.9362, and 0.7413–0.8516 with Petaling basins. Besides, the fractal dimensions of the basin-wise channel networks (Fig. 4c, d) extracted from DEMs of Cameron Highlands and Petaling regions also indicate a clear distinction between these two regions (see last column of Table 2). Fractal dimensions of these networks are calculated using the box-counting method, where extracted networks of both DEMs are taken as foreground objects. It is noticed from Fig. 4c, d that Petaling sub-basins have a sparser network in comparison to the intricate denser network found in Cameron sub-basins. This observation is reflected in the fractal dimensions in Cameron basins (1.3192–1.5814) and Petaling (1.1706–1.314) basins. Fig. 7a, b show a better view of the relationships among these various parameters. From these graphs, we can infer that Cameron basins, which have higher altitude basins than do low-lying Petaling basins, show higher drainage densities and convexity measures (whether Horton, method-1, or method-2), higher normalized complexity measures, and also higher fractal dimension values than do Petaling basins. Besides, unlike the case of synthetic basin and fractal basin functions, the convexity measures obtained from methods-1 and -2 with Cameron and Petaling basins correspond well with the Horton drainage density. Furthermore, it is interesting to note from Fig. 7b that the convexity measure from method-1 follows closely the Horton drainage density. Hence, we conjecture that our proposed methods-1 and -2 offer alternative ways to quantitatively characterize basins, complementing already existing quantitative geomorphometric techniques.

## 5. Conclusion

Factors such as climate, soil permeability, and several other hydrologically relevant parameters affect geomorphological processes within a basin, besides physical characteristics including relief levels. In this paper, we investigate the changes in convexity measures due to different elevation ranges of basins with similar

geometrical arrangement. From our results, it is conspicuous that planimetric based Hortonian drainage density is of limited use. Our proposed function-based convexity measures not only could capture the spatial variability between basins with different altitudes, but they are also appropriate quantitative geomorphometric parameters. Many quantitative geomorphometric parameters derived from conventional map-based feature analysis are terrain independent, whereas our proposed convexity measures, which are computed through these function-based approaches are clearly terrain dependent. An interesting open problem is that of validation of the relationship between these convexity measures of realistic basins that possess different physiographic set-ups. In summary, we provide a method/approach to estimate the convexity measure of a basin when it is considered to be a function rather than a set. These convexity measures, which are related to fractals and granulometric analysis, derived via geometry-based techniques, provide new insights to the exploration of further links with various other established and to be derived parameterized morphometric measures. The study on the drawing of scale-invariant characteristics from these convexity measures has a potential scope in this investigation.

## References

- Band, L.E., 1993. Extraction of drainage networks and topographic parameters from digital elevation data, Channel Network Hydrology. Wiley, pp. 13–42.
- Chockalingam, L., Sagar, B.S.D., 2005. Morphometry of networks and non-network spaces. Journal of Geophysical Research 110, B08203.
- Horton, R.E., 1945. Erosional development of streams and their drainage basins: hydrological approach to quantitative morphology. Bulletin of the Geophysical Society of America 56, 275–370.
- Howard, A.D., 1997. Badland morphology and evolution: interpretation using a simulation model. Earth Surface Processes Landforms 22, 211–227.
- Jenson, S.K., Domingue, J.O., 1988. Extraction of topographic structures from digital elevation data and geographic information system analysis. Photogrammetric Engineering and Remote Sensing 54 (11), 1593–1600.
- Kirkby, M.J., 1993. Long term interactions between networks and hillslopes, Channel Network Hydrology. John Wiley, New York, pp. 255–293.
- Kirkby, M.J., 1980. The stream head as a significant geomorphic threshold, Thresholds in Geomorphology. Allen and Unwin, London, pp. 53–73.
- Lim, S.L., Sagar, B.S.D., 2008. Cloud field segmentation via multiscale convexity analysis. Journal of Geophysical Research 113 (D13208). doi:10.1029/2007JD009369.
- Lindsay, J.B., 2005. The terrain analysis system: a tool for hydro-geomorphic applications. Hydrological Processes 19, 1123–1130.
- Mandelbrot, B.B., 1982. The Fractal Geometry of Nature. Freeman, San Francisco, California.
- Maragos, P., 1989. Pattern spectrum and multiscale shape representation. IEEE Transactions on Pattern Analysis and Machine Intelligence 11 (7), 701–716.
- Marani, M., Belluco, E., D'Alpaos, A., Defina, A., Lanzoni, S., Rinaldo, A., 2003. On the drainage density of tidal network. Water Resources Research 39 (2), 4.1–4.11. doi:10.1029/2001WR001051.
- Montgomery, D.R., Dietrich, W.E., 1994. Landscape dissection and drainage area-slope thresholds, Process Models and Theoretical Geomorphology. John Wiley, New York, pp. 221–246.
- Montgomery, D.R., Dietrich, W.E., 1989. Source areas, drainage density, and channel initiation. Water Resources Research 25 (8), 1907–1918.
- O'Callaghan, J.F., Mark, D.M., 1984. The extraction of drainage networks from digital elevation data. Computer Vision, Graphics, and Image Processing 28, 323–344.
- Sagar, B.S.D., Srivinas, D., Rao, B.S.P., 2001. Fractal skeletal based channel networks in a triangular initiator basin. Fractals 9 (4), 429–437.
- Sagar, B.S.D., Tien, T.L., 2004. Allometric power-law relationships in a Hortonian Fractal DEM. Geophysical Research Letters 31 (6), L06501.
- Sagar, B.S.D., Venu, M., Srivinas, D., 2000. Morphological operators to extract channel networks from digital elevation models. International Journal of Remote Sensing 21 (1), 21–30.
- Schumm, S.A., Mosley, M.P., Weaver, W.E., 1987. Experimental Fluvial Geomorphology. John Wiley, New York.
- Serra, J., 1982. Image Analysis and Mathematical Morphology. Academic Press, London.
- Soille, P., 1998. Gray scale convex hulls: definition, implementation and application. In: Proceedings of the ISMM' 98, Kluwer Academic Publishers.
- Strahler, A.N., 1964. Quantitative geomorphology of drainage basins and channel networks. In: Chow, V.T. (Ed.), Handbook of Applied Hydrology. McGraw-Hill, New York.
- Tarboton, D.G., 1997. A new method for the determination of flow direction and contributing area in grid digital elevation models. Water Resources Research 33 (2), 309–319.

- Tarboton, D.G., Ames, D.P., 2001. Advances in the mapping of flow networks from digital elevation data. World Water and Environmental Resources Congress May, 20–24 Orlando, Florida.
- Tarboton, D.G., Bras, R.L., Rodriguez-Iturbe, I., 1991. On the extraction of channel network from digital elevation data. *Hydrological Processes* 5, 81–100.
- Tarboton, D.G., Bras, R.L., Rodriguez-Iturbe, I., 1992. A physical basis for drainage density. *Geomorphology* 5 (1–2), 59–76.
- Tay, L.T., Sagar, B.S.D., Chuah, H.T., 2007. Granulometric analyses of basin-wise DEMs: a comparative study. *International Journal of Remote Sensing* 28 (15), 3363–3378.
- Tucker, G.E., Bras, R.L., 1998. Hillslope processes, drainage density, and landscape morphology. *Water Resources Research* 34 (10), 2751–2764.
- Tucker, G.E., Catani, F., Rinaldo, A., Bras, R.L., 2001. Statistical analysis of drainage density from digital terrain data. *Geomorphology* 36, 187–202.